

SIGNATURE OF GALACTIC OUTFLOWS AS ABSORPTION-FREE GAPS IN THE LY $\alpha$  FORESTTAOTAO FANG<sup>1</sup>, ABRAHAM LOEB<sup>2</sup>, DAVID TYTLER<sup>3</sup>, DAVID KIRKMAN<sup>3</sup>, AND NAO SUZUKI<sup>3</sup>  
*Draft version September 5, 2018*

## ABSTRACT

Powerful outflows from star-forming galaxies are expected to push away the neutral intergalactic medium (IGM) around those galaxies, and produce absorption-free gaps in the Ly $\alpha$  forest. We analyze the abundance of gaps of various sizes in three high resolution spectra of quasars at  $z \sim 3 - 3.5$ . The gap statistics agrees well with a model in which galactic halos above a minimum mass scale of  $M_{\min} \sim 10^{10} M_{\odot}$  produce bubbles with a characteristic radius of  $R_b \sim 0.48 h^{-1}$  Mpc. Both numbers are consistent with naive theoretical expectations, where the minimum galaxy mass reflects the threshold for infall of gas out of a photo-ionized IGM. The observed gaps are typically bounded by deep absorption features as expected from the accumulation of swept-up gas on the bubble walls.

*Subject headings:* large-scale structure of the universe — intergalactic medium — quasars: absorption lines — cosmology: theory

## 1. INTRODUCTION

The formation and evolution of galaxies is regulated by their feedback on the surrounding intergalactic medium (IGM). Radiative feedback owing to photo-ionization heating by a cosmic UV background or hydrodynamic feedback owing to outflows driven by supernovae or quasars, can suppress the infall of IGM gas onto low-mass dark-matter halos (see, e.g., Ikeuchi 1986; Rees 1986; Babul & Rees 1992; Efstathiou 1992; Thoul & Weinberg 1996; Scappaticcio & Oh 2004). The feedback introduces a minimum halo mass above which halos can efficiently accrete gas from the IGM and host star formation or quasar activity. Infall of gas is suppressed if the gravitational potential well of a halo is shallow, explaining why dwarf galaxies have a much lower abundance than expected for low-mass halos (e.g., White & Frenk 1991; Kauffmann, White, & Guiderdoni 1993).

In this *Letter*, we examine a simple observational method to reveal the scars left by hydrodynamic outflows from galaxies on the IGM. Powerful outflows from galaxies are expected to push away the neutral intergalactic medium (IGM) around those galaxies, and produce absorption-free gaps in the Ly $\alpha$  forest towards a background quasar (Theuns et al. 2001). Studies of the Ly $\alpha$  forest — the narrow absorption lines produced by intergalactic neutral hydrogen in quasar spectra — had been very successful in mapping large scale structure in the universe at high redshift (for a review, see Rauch 1998). While the IGM dynamics is shaped by gravity alone on large scales (see, e.g., Cen et al. 1994; Hernquist et al. 1996; Meiksin & White 2001; McDonald et al. 2004), outflows can play an important role on small scales by introducing gaps in the Ly $\alpha$  forest that can be identified in high resolution observations of quasar spectra.

Our model is simple: an outflow from a galaxy evacuates a bubble in the IGM, leaving behind little or no neutral hydrogen as the swept-away gas piles up on the bubble

surface. Such a bubble would appear as a gap in the Ly $\alpha$  forest absorption spectrum of a background quasar, i.e., a flat spectral segment with little or no absorption. The expected distribution of absorption-free gaps can be calculated from the number density of halos above the minimum mass, as only those halos are capable of hosting supernova or quasar-driven outflows. For the halo mass range of interest,  $\sim 10^9 - 10^{11} M_{\odot}$ , the bubble radius is expected to be almost independent of halo mass at a given redshift (Furlanetto & Loeb 2003). Hence, our analytic model has only two free parameters: the minimum halo mass for the production of outflows,  $M_{\min}$ , and the characteristic bubble radius  $R_b$  for halos above that mass.

There have already been some observational reports about the signatures of outflows around massive starburst galaxies (with  $M \gg M_{\min}$ ) at high redshifts. Shapley et al. (2003) discovered large scale outflows with velocities up to  $\sim 600 \text{ km s}^{-1}$  by studying  $\sim 10^3$  Lyman Break Galaxies (LBGs) at  $z \sim 3$ . Using a large sample of quasar spectra which pass by foreground LBGs, Adelberger et al. (2003) identified the lack of neutral hydrogen within  $\sim 0.5 h^{-1}$  comoving Mpc around LBGs. Recent observations of high redshift, submillimeter galaxies also indicated the existence of large scale outflows (see, Genzel et al. 2004 and reference therein). The properties of active bubbles around starburst galaxies may be different than those of mature bubbles around more common galaxies for which the wind material had sufficient time to accumulate on the bubble walls and decelerate after evacuating the bubble interior. In simulations, Croft et al. (2002) and Kollmeier et al. (2003) also found absorption-free gaps in their simulated Ly $\alpha$  spectrum caused by galactic winds. Our goal in this *Letter* is to characterize the properties of the typical relic bubbles around the most common ( $M \sim M_{\min}$ ) galaxies at redshift  $z \sim 3$ .

Our paper is organized as follows. In §2 we briefly describe our analytic model and derive its basic equations. In §3 we compare the model with three high-resolution

<sup>1</sup> Department of Astronomy, University of California, Berkeley, CA 94720; Chandra Fellow<sup>2</sup> Astronomy Department, Harvard University, 60 Garden Street, Cambridge, MA 02138<sup>3</sup> Center for Astrophysics and Space Sciences, University of California, San Diego, MS 0424, La Jolla, CA 92093

quasar spectra. Finally, we conclude with a discussion about the assumptions of our model and the implications of our results. Throughout the paper, we assume the concordance cosmological model with  $\Omega_M = 0.27$ ,  $\Omega_\Lambda = 0.73$ ,  $\Omega_b = 0.044$ ,  $h = 0.71$ , and  $\sigma_8 = 0.84$  determined by recent WMAP data (Spergel et al. 2003).

## 2. MODEL

In our simple model, a galactic wind sweeps-up the surrounding intergalactic medium and eliminates HI absorption within a bubble radius  $R_b$  of order a few hundred kpc (Adelberger et al. 2003; Furlanetto & Loeb 2003). The bubble spends most of the time approaching a fixed comoving distance from its host galaxy, at which the (decelerating) expansion speed asymptotes to the local Hubble velocity (see section SS4). Such a bubble would produce a gap in the Ly $\alpha$  forest imprinted on the spectrum of a background quasar. The absorption-free gap should have a high value of the mean transmission  $F$  [defined as  $\exp(-\tau)$  where  $\tau$  is the optical depth] that is close to unity. Our goal is to calculate the expected size distribution of such gaps in the Ly $\alpha$  forest and compare it with observations.

Given a comoving density of halos per unit mass of  $dn_h(M)/dM$  and the assumption that the wind from each halo of mass  $M$  produces bubble of a comoving radius of  $R_b(M)$ , the probability of finding an absorption-free gap (with  $F \sim 1$ ) of comoving size in the range between  $L$  and  $L + dL$  per infinitesimal comoving path-length,  $dl$ , is given by

$$\frac{dP}{dL dl} = \int_{M_{min}} \frac{dn_h}{dM} \frac{d\sigma}{dL} dM. \quad (1)$$

Here,  $\sigma = \pi b^2$  is the cross-section of the bubble for an impact parameter  $b = \sqrt{R_b^2 - (L/2)^2}$ , and  $M_{min}$  is the minimum halo mass into which IGM gas accretes efficiently. The differential cross-section for having a bubble segment of length between  $L$  and  $L + dL$  is then,

$$\frac{d\sigma}{dL} = \begin{cases} \pi L/2 & 0 < L < 2R_b(M); \\ 0 & L \geq 2R_b(M) \end{cases} \quad (2)$$

The expected number of absorption-free gaps with a size larger than  $L$  is

$$\begin{aligned} \frac{dP}{dl}(\geq L) &= \int_{M_{min}}^{\infty} \int_L^{2R_b(M)} \frac{dn_h}{dM} \frac{d\sigma}{dL'} dL' dM \\ &= \int_{M_{min}}^{\infty} \pi \left( R_b^2 - \frac{L^2}{4} \right) \frac{dn_h}{dM} dM. \end{aligned} \quad (3)$$

Since  $R_b(M)$  has a rather weak dependence on  $M$  across the relevant range of halo masses (see Fig. 1 in Furlanetto & Loeb (2003)), we assume for simplicity a single value for  $R_b$  when fitting observational data at a given redshift. We adopt the Press & Schechter (1974) mass function of halos and use  $M_{min}$  as the second adjustable parameter. The concordance cosmological model yields the following values for the cumulative number density:  $n_h(> M_{min}) = 1, 0.1$ , and  $0.01 h^3$  comoving Mpc $^{-3}$ , for  $M_{min} = 1.3 \times 10^9, 1.2 \times 10^{10}$ , and  $10^{11} M_\odot$ , respectively. Figure 1 shows results from equation (3) for the three cases of  $M_{min} = 1.3 \times 10^9 M_\odot$  (dashed line),  $M_{min} = 1.2 \times 10^{10} M_\odot$  (dotted line), and  $M_{min} = 10^{11} M_\odot$  (solid line).

## 3. OBSERVATIONS

### 3.1. Data Analysis

Next, we apply our analytic method to three high-resolution, high signal-to-noise ratio ( $S/N$ ) spectra: Q 1422+231 at  $z = 3.62$  (Rauch et al. 2001); Q 0130-4021 at  $z = 3.023$  and Q 0741+4741 at  $z = 3.21$  (Kirkman et al. 2000, 2005). These quasar were observed with the Keck High Resolution Echelle Spectrometer (HIRES), at  $S/N$  of  $\gtrsim 50 - 70$ . The resolution for Q 1422+231 is  $\sim 23.3 h^{-1}$  kpc, and for the other two is  $\sim 8 \text{ km s}^{-1}$ . We refer readers to Rauch et al. (2001) and Kirkman et al. (2005) for details of continuum fitting. By fit artificial spectra for 24 QSOs, Kirkman et al. (2005) measured a typical error in continuum level of 1.2%. The actually error in our sample should be much smaller due to the higher  $S/N$ .

We select a portion of the spectrum around  $z \sim 3$  to test our analytic model. Specifically, we consider the observed wavelength band of  $4500 \leq \lambda \leq 4800 \text{ \AA}$ , corresponding to a comoving path length of  $\sim 180 h^{-1}$  Mpc. For Q 0130-4021 and Q 0741+4741, only Ly $\alpha$  absorption presents in this wavelength range, while for Q 1422+231, Ly $\beta$  will cover part of this range (but not Ly $\gamma$ ) and will have quite a bit more absorption. We split the spectrum into segments with a size of  $60 h^{-1}$  Mpc each so that we have a total of 9 segments for the entire sample. We then normalize each of the 9 segments separately. We did this by varying the optical depth  $\tau$  so that the mean flux  $\bar{F} = 0.684$ , consistent with the observed value at  $z = 3$  (McDonald et al. 2000; Kirkman et al. 2005). We did not vary the normalization with wavelength. We measure gaps in each segment, and the errors are estimated by using the variance between these 9 subsamples.

We directly measure  $dP/dl(\geq L)$  from the observed spectrum. The flat absorption-free gaps are selected by searching for segments with transmission  $F \geq F_{th}$  where  $F_{th} = 0.99$  is our fiducial threshold. Other choices of the threshold transmission may be considered plausible, since Adelberger et al. (2003) found that the mean transmitted flux is  $> 0.8$  within  $0.5 h^{-1}$  comoving Mpc of the LBGs and possibly higher close to the LBGs. Note that since LBGs are selected by having ongoing starburst activity, their active wind may add some absorption by outflowing material inside their bubbles. Other galaxies are most likely to be surrounded by empty relic bubbles bounded by a thin shell of swept-up gas, long after their powerful starburst activity has ended. However, a low value of  $F_{th}$  is very likely to mix the outflow-driven bubbles discussed here with high-transmission gaps caused by gravitationally-induced voids (which are underdense but not completely empty). We have chosen the threshold of 0.99 based on a detailed analysis of the results of a numerical simulation from a Particle-Mesh (PM) code involves gravity only (see, e.g., Meiksin & White 2003; White 1999). We found that the PM simulation provides the same distribution of gaps as the data up to a threshold of  $\sim 0.97$ , and the data shows a clear over-abundance of gaps at a threshold of 0.99: at  $F_{th} = 0.99$  the gravity-induced gaps accounts for less than  $\sim 10\%$  of the total gaps found in the observation data.

In principle we could have used the raw spectrum, the noise in each pixel generates artificial gaps with a width of just a few pixels. Instead, we use the fitted spectrum,

which smoothes out these random pixel noise. Using high-order statistic method, Fang & White (2004) found that the coherence scale length of spatial correlation in Keck data must be smaller than  $0.3h^{-1}$  Mpc, which roughly corresponds to 12 pixels in the spectrum. So the raw spectrum is smoothed by the boxcar method with a width of 12 pixels to ensure that we can smooth Poisson noise in each pixel but preserve the large scale features. The  $1-\sigma$  error bars are obtained directly from Poisson statistics.

We fit the observed distribution of gap sizes using equation (3), with two free parameters:  $M_{\min}$  and  $R_b$ . We use a least- $\chi^2$  analysis with

$$\chi^2 \equiv \sum_i [y(M_{\min}, R_b) - y_i]^2 / \sigma_i^2. \quad (4)$$

Here  $y(M_{\min}, R)$  is the expected value of  $dP/dl$  based on equation (3),  $y_i$  is the observed value of  $dP/dl$ , and  $\sigma_i$  is the  $1-\sigma$  error for each data point. The  $\chi^2$  fit yields the best-fit parameters of  $M_{\min} = 1.2 \times 10^{10} M_{\odot}$  and  $R_b = 480 h^{-1}$  comoving kpc, with a  $\chi^2$  value of 1.2 per degree-of-freedom. The model fits the observation data well between 0.1 and  $1 h^{-1}$  Mpc<sup>4</sup>, as indicated by the red solid line in Figure 1.

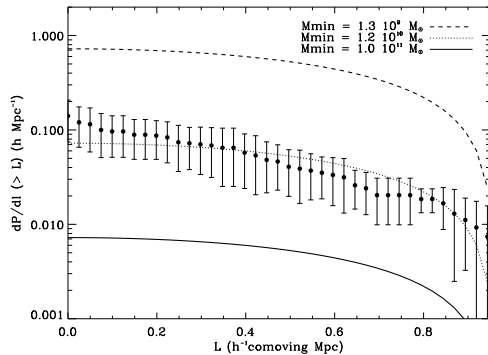


FIG. 1.— Cumulative distribution of absorption-free gaps with comoving length  $> L$  per comoving  $h^{-1}$  Mpc. The three heavy lines show results from our a  $0.48 h^{-1}$  Mpc and different value of  $M_{\min}$ . Data is shown as points (extracted with  $F_{th} = 0.99$ ) with  $1-\sigma$  Poisson error bars. The middle dashed is our best-fit model.

### 3.2. Results

The best-fit value for the minimum halo mass that is capable of hosting outflows (due to star formation or quasar activity), is consistent with the value expected from hydrodynamic simulations and semi-analytic analysis. The mass of a dark matter halo is related to its circular velocity  $V_{circ}$  and collapse redshift  $z_c$  ( $\gg 1$ ),

$$M = 10^{10} M_{\odot} \left( \frac{V_{circ}}{50 \text{ km s}^{-1}} \right)^3 \left( \frac{1+z_c}{4} \right)^{-\frac{3}{2}}. \quad (5)$$

The infall of gas onto dwarf galaxies is significantly suppressed through photoionization heating of the IGM by the cosmic ultraviolet background radiation after cosmological reionization (Rees 1992; Efstathiou 1992; Thoul & Weinberg 1996). As soon as the IGM is heated to a temperature of  $1-2 \times 10^4$  K, its thermal pressure suppresses gas infall into shallow gravitational potential wells. The minimum halo mass due to photo-ionization heating corresponds to a virial temperature of  $\sim 10^5$  K. The reason is

<sup>4</sup> The correlation function of galaxy halos of  $\sim 10^{10} M_{\odot}$  at  $z \sim 3$  implies that the chance for overlap of bubbles with a radius  $480 h^{-1}$  comoving kpc around these galaxies, is small in our data set.

that photo-ionization heats the IGM to  $\sim 10^4$  K but when the gas virializes into a halo, its density increases by a factor of  $\sim 200$  and so its temperature rises adiabatically by a factor  $\sim 200^{2/3} \sim 35$ . Only if this final temperature is below the virial temperature, will the gas condense by this factor of  $\sim 200$ . The minimum halo mass for galaxies is defined as the threshold where  $\sim 50\%$  of the baryons that were supposed to condense made it. This gives a minimum virial temperature of  $\sim 10^5$  K. The corresponding minimum circular velocity of the halo is (Barkana & Loeb 2001),

$$V_{min} = 60 (T/10^5 \text{ K})^{\frac{1}{2}} \text{ km s}^{-1}. \quad (6)$$

Detailed hydrodynamic simulations (e.g., Thoul & Weinberg 1995, 1996; Navarro & Steinmetz 1997; Dijkstra et al. 2004) confirm this value, showing that at redshift  $z = 3$  only  $\sim 50\%$  of the available gas accretes onto halos with  $V_{circ} \sim 50 \text{ km s}^{-1}$ , and the infall of gas onto halos with  $V_{circ} \leq 25-30 \text{ km s}^{-1}$  is completely suppressed. This yields a minimum halos mass of  $\sim 10^{10} M_{\odot}$  based on equation (5), in agreement with the value derived from the statistics of absorption-free gaps in the Ly $\alpha$  forest.

The typical bubble radius  $R_b$  we derived is consistent with both semi-analytic analysis and other observations. Based on a starburst wind model, Furlanetto & Loeb (2003) showed that at redshift  $z \sim 3$  and halos with masses between  $\sim 3 \times 10^8 M_{\odot}$  and  $10^{10} M_{\odot}$ , the physical (proper) radius  $R_b/(1+z)$  ranges between  $\sim 50$  to  $\sim 100$  kpc (see the upper left panel of their Fig. 1). For halo masses above  $10^{10} M_{\odot}$ , the maximum radius can be achieved by the wind is nearly constant,  $\sim 100$  kpc. Observations indicate the lack of H I within a radius of 500 comoving kpc around LBGs, which translates to  $\sim 125$  proper kpc at  $z = 3$  (Adelberger et al. 2003), although the interpretation may be complicated (Kollmeier et al. 2003).

### 4. DISCUSSION

The gas that is swept-up from the bubble volume by a galactic outflow, is expected to pile-up in a thin shell on the bubble wall, and introduce enhanced absorption at both ends of its absorption-free segment in the Ly $\alpha$  forest (Furlanetto & Loeb 2003). Indeed, the spectrum of Q 1422+231 indicates that almost all of the flat transmission segments have deep absorption features at one or both of their boundaries. Figure 2 shows four examples of absorption-free segments with enhanced absorption at both ends. In all panels, the upper dotted horizontal line show the flux threshold  $F_{th} = 0.99$ , and the lower horizontal line indicates the mean transmitted flux of  $\bar{F} = 0.684$  at  $z \sim 3$  (bottom). We note that in analogy with supernova remnants (Chevalier, Blondin, & Emmering 1992), the shell of the swept-up material may fragment into clumps due to convective or Rayleigh-Taylor instability. In such a case, a flat (absorption-free) segment would be bounded by a narrow, deep absorption feature only if the line-of-sight happens to cross a clump of gas. We find that out of 23 absorption-free segments with  $L > 0.1 h^{-1}$  Mpc, 6 are bounded at both ends by deep absorption features extending under  $\bar{F}$ , 12 have such a feature at one end, and only

5 are not bounded at all by a flux depression under  $\bar{F}$ . There is tentative evidence for clumpiness of the bubble walls, although the last class of segments may also receive a contribution from ionization (Strömgren) spheres around bright galaxies.

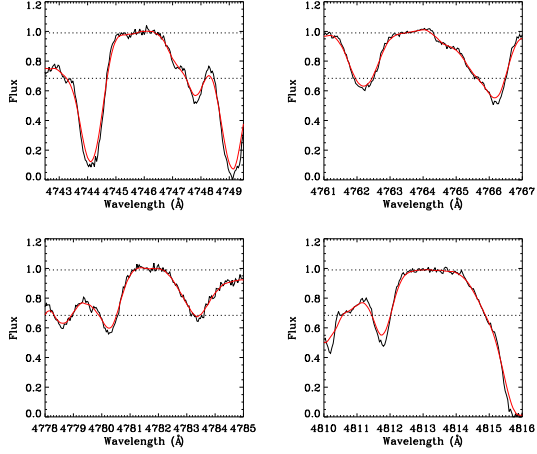


FIG. 2.— Four examples of absorption-free segments in the spectral interval between 4740Å and 4820Å of Q 1422+231. The raw data is indicated by the black fluctuating lines and the smoothed spectra are delineated by the red smooth curves. In each panel, the top horizontal dotted line marks the threshold  $F_{th} = 0.99$  and the bottom horizontal line indicates the *mean* transmitted flux at  $z \sim 3$ . All four examples show enhanced absorption at the two edges of the central flat (absorption-free) segment, as expected from the pile-up of hydrogen on the surface of the associated bubbles. Some absorption-free segments (not shown here) are not bounded by deep absorption features at both ends, indicating clumpiness of the bubble material.

Our analysis assumed that the bubble size can be translated to the spectral width of the absorption-free gaps for a pure Hubble flow, and ignored the possible effects peculiar velocities. In reality, the spectral width may be increased due to the bubble expansion relative to the local Hubble flow. This would tend to increase the inferred value of  $R_b$  relative to its true physical size. The local hubble flow at  $z \sim 3$  is  $v_h \sim 32 \text{ km s}^{-1}$  for bubbles with a radius of  $\sim 100$

proper kpc. The upper left panel of Figure 2 in Furlanetto & Loeb (2003) shows that for most halos with halo mass between  $10^9$ – $10^{10} M_\odot$  the average bubble expansion velocity is around  $v_{exp} \sim 40 \text{ km s}^{-1}$ . Since the peculiar velocity,  $(v_{exp} - v_h)$ , is much smaller than the hubble flow  $v_h$ , we can safely ignore its contribution to the broadening of the flat spectral segments. On the other hand, neutral hydrogen outside the bubble may also have effect in translating the bubble size into the spectral width of the gap, depending on whether the bubble is expanding into an infall region (surrounding an overdense environment) or an outflow region (in a locally underdense region): the infall can require the true physical bubble size to be larger (see, e.g., Kollmeier et al. 2003).

In this *Letter* we have only attempted to demonstrate the feasibility of our method at  $z \sim 3$ . The statistical significance of our results can be enhanced through the analysis of additional data sets of high-resolution quasar spectra. We also need better calibrated data, with accurate continuum level, and more realistic simulations. In the future, our method can be used to measure the variation of  $M_{\min}$  and  $R_b$  with redshift, and to gauge the impact of galaxy feedback on estimates of the dark matter power-spectrum on small scales.

Quasar spectra were based on data obtained at the W.M. Keck Observatory, a joint facility of the University of California, the California Institute of Technology, and NASA. We thank M. Rauch and W. Salgert for providing Keck data of QSO 1422+231, and M. White for providing PM simulation data. T. Fang was supported by NASA through the *Chandra* Postdoctoral Fellowship Award Number PF3-40030 issued by the *Chandra* X-ray Observatory Center, which is operated by the Smithsonian Astrophysical Observatory for and on behalf of the NASA under contract NAS8-39073. This work was supported in part by NASA grant NAG 5-13292, and by NSF grant AST-0204514 (for A.L.). DT and DK were supported in part by NSF grant AST-0098731 and NASA grants NAG5-13113 and STScI grant HST-AR-10288.01-A.

## REFERENCES

Adelberger, K. L., Steidel, C. C., Shapley, A. E., & Pettini, M. 2003, *ApJ*, 584, 45  
 Babul, A. & Rees, M. J. 1992, *MNRAS*, 255, 346  
 Barkana, R. & Loeb, A. 2001, *Physics Report* (astro-ph/0010468)  
 Cen, R., Miralda-Escude, J., Ostriker, J. P., & Rauch, M. 1994, *ApJ*, 437, L9  
 Chevalier, R. A., Blondin, J. M., & Emmering, R. T. 1992, *ApJ*, 392, 118  
 Croft, R. A. C., Hernquist, L., Springel, V., Westover, M., & White, M. 2002, *ApJ*, 580, 634  
 Dijkstra, M., Haiman, Z., Rees, M. J., & Weinberg, D. H. 2004, *ApJ*, 601, 666  
 Efstathiou, G. 1992, *MNRAS*, 256, 43  
 Fang, T., & White, M. 2004, *ApJ*, 606, L9  
 Furlanetto, S. R. & Loeb, A. 2003, *ApJ*, 588, 18  
 Genzel, R. et al. 2004, to appear in the proceedings of the Venice conference "Multiwavelength Mapping of Galaxy Formation and Evolution" (astro-ph/0403183)  
 Hernquist, L., Katz, N., Weinberg, D. H., & Miralda-Escude, J. 1996, *ApJ*, 457, L51  
 Ikeuchi, S. 1986, *Ap&SS*, 118, 509  
 Kauffmann, G., White, S. D. M., & Guiderdoni, B. 1993, *MNRAS*, 264, 201  
 Kirkman, D., Tytler, D., Burles, S., Lubin, D., & O'Meara, J. M. 2000, *ApJ*, 529, 655  
 Kirkman, D., et al. 2005, *MNRAS*, accepted (astro-ph/0504391)  
 Kollmeier, J. A., Weinberg, D. H., Davé, R., & Katz, N. 2003, *ApJ*, 594, 75  
 Meiksin, A., & White, M. 2003, *MNRAS*, 342, 1205  
 Meiksin, A., & White, M. 2001, *MNRAS*, 324, 141  
 McDonald, P., Miralda-Escudé, J., Rauch, M., Sargent, W. L. W., Barlow, T. A., Cen, R., & Ostriker, J. P. 2000, *ApJ*, 543, 1  
 McDonald, P., et al. 2004, *ApJ*, submitted (astro-ph/0405013)  
 Navarro, J. F. & Steinmetz, M. 1997, *ApJ*, 478, 13  
 Peebles, P. J. E. 1993, *Princeton Series in Physics*, Princeton, NJ: Princeton University Press, —c1993.  
 Press, W. H. & Schechter, P. 1974, *ApJ*, 187, 425  
 Rauch, M. 1998, *ARA&A*, 36, 267  
 Rauch, M., Sargent, W. L. W., Barlow, T. A., & Carswell, R. F. 2001, *ApJ*, 562, 76  
 Rees, M. J. 1986, *MNRAS*, 218, 25P  
 Rees, M. J. 1992, *MNRAS*, 218, 25  
 Scannapieco, E. & Oh, S. P. 2004, *ApJ*, accepted (astro-ph/0401087)  
 Shapley, A. E., Steidel, C. C., Pettini, M., & Adelberger, K. L. 2003, *ApJ*, 588, 65  
 Spergel, D. N., et al. 2003, *ApJS*, 148, 175  
 Theuns, T., Mo, H. J., & Schaye, J. 2001, *MNRAS*, 321, 450  
 Thoul, A. A & Weinberg, D. H. 1995, *ApJ*, 442, 480  
 Thoul, A. A & Weinberg, D. H. 1996, *ApJ*, 465, 608  
 White, S. D. M. & Frenk, C. S. 1991, *ApJ*, 379, 52  
 White, M. 1999, *MNRAS*, 310, 511